Journal of Mechanical Engineering and Sciences
ISSN (Print): 2289-4659; e-ISSN: 2231-8380
Volume 11, Issue 2, pp. 2637-2649 June 2017

DOI: https://doi.org/10.15282/jmes.11.2.2017.7.0241

Crushing behaviour of composite square honeycomb structure: a finite element analysis

Z. Ansari[1], C.W. Tan [1], M.R.M. Rejab[1], D. Bachtiar[1], J. Siregar[1], M.Y.M. Zuhri[2] and N.S.D.M. Marzuki[1]

[1]Structural Materials & Degradation Focus Group, Faculty of Mechanical Engineering, Universiti Malaysia Pahang, 26600 Pekan, Pahang, Malaysia
[2]Faculty of Engineering, Universiti Putra Malaysia,
43400 UPM Serdang, Selangor, Malaysia.
Phone: +6094246255; Fax: +6094246222
*Email: zahidah.engineer@gmail.com

ABSTRACT

This paper investigates the compression properties of square honeycomb core materials based on glass fibre reinforced plastic. The objective of this project is to determine the failure strength and energy absorption of the square honeycomb structure and compare both crushing behaviours between the experimental and finite element simulations. Control specimen made from GFRP is prepared by using traditional hand lay-up technique and the mechanical properties are determined from the INSTRON Tensile Machine. In this study, the numerical simulation of the square honeycomb structure is analysed with the commercial software. In this simulation, the result obtained for maximum stress is 28.24MPa which is located at node 110451. Besides that, the energy absorption for finite element result and experimental result are 310.86 kJ and 282.17 kJ, respectively. The percentage of error is 9.23% which can be considered a good agreement between numerical simulation and experimental result. Lastly, the crushing behaviour between the finite element model and experimental model is slightly different to each other since the model in simulation is assumed to be the preferred structure, whereas the experimental model is imperfect in the geometric model.

Keywords: Honeycomb square; crushing behavior; energy absorption.

INTRODUCTION

In year 2010, 414 421 cases of road accidents occurred in Malaysia. 28269 cases were involved in road casualties and 6872 cases resulted in road deaths. The cases of road accidents in Malaysia were showing an increasing trend every year. Malaysian road users are classified as the worst in Sounth East Asia with an average of 23.8 deaths per 100,000 populations over the span of 12 years, according to the World Health Organisation's (WHO) Global Status Report. In order to reduce road accidents, transportation and vehicle manufacturers are searching for an advanced buffer structure that has low weight and volume to design the vehicle [1]. The advanced buffer structure found is the honeycomb structure. Honeycomb structures are used as shock- absorbent layers in an automobile because of the anti-shock properties and high energy absorption to reduce the impact effect [2, 3]. Honeycomb structures have a minimum amount of material used to achieve minimum weight and material cost. Honeycomb structures are widely used in

various distinct engineering fields including in the automotive and aerospace industries. The honeycomb material can easily function as tailored solutions due to its unique design of connecting the network of the structure [4-7]. Besides that, the main advantages of the honeycomb structures are light-weight, low density, high stiffness to weight ratio, high energy absorption and great anti-shock properties [8] , [9]. In this project, the square honeycomb structure is chosen because of the high energy absorption properties with minimum peak stress values compared to hexagonal and triangular honeycomb structures [10]. Besides that, the composite material is chosen because of the high strength to weight ratio, lightweight and fire resistance as well its wide usage in various sectors nowadays.

A composite is a material having two or more distinct materials that are combined together on a microscopic scale to form an outstanding third material [11]. The composite in this study is made up of two materials which are matrix and glass fibre reinforcement [12-15]. Each material has significant distinct chemical and physical properties. Therefore, when the materials are combined, it forms a unique and superior material that has stronger and lighter materials compared to the original materials. Lately, composites are also known as reinforced plastics. Composite materials are the new products of the so-called advanced engineering age [2, 16-19]. Fibres in composites are held together by a binder known as matrix. Polymers used as matrix materials are referred to as resin [20]. There are two different types of resins which are thermoplastic and thermosets. The difference between the two resins is their behaviour when heated. However, only thermosets resin is focused on in this study. The three primary functions of the resin are [21]:

a. Support the fibres and transfer the stress to ensure the fibres can carry more loads.
b. Protect the fibres from physical damage before and during structure fabrication.
c. Increase the toughness and ductility of the resin to reduce the propagation of cracks in the composite.

Thermoset resins are usually used in liquid form. Thermosets are made up of a three-dimensional cross-linked structure. Therefore, when undergoing chemical reactions, the entire polymer chains are connected to the matrix in a three-dimensional network. The benefits of thermosets are good resistance to solvents and temperature. Thermosets undergo an irreversible process when heated. Thermosets consist of two types of resins which are Polyester and Epoxy. Polyesters are used extensively with glass fibre [5, 18, 22]. They are inexpensive and light with a temperature range of up to 100°C and resistant to environmental exposure, whereas epoxy is more expensive but has better moisture resistance and lower shrinkage on curing. However, only polyester resin is focused on in this study.

Polyester resins are an unsaturated synthetic resin that is formed by reactions of polyhydric alcohols and dibasic organic acids. Unsaturated polyester resin is a thermoset resin which can be cured by a liquid or solid state when put into the right conditions. Polyesters are made from different acids, glycols, and monomers, and each of the molecules has different properties [23-25]. Polyester is a polymers category that contains the ester functional group in its main chain. Polyester resins are the most widely and commonly used resin in the marine industry, aircraft industry and structural parts of the automobile [26]. Glass fibre reinforced composites can be divided into two typical types of fabric which are chopped strand mat and woven roving [2, 17, 25]. Chopped strand mat (CSM) is a discontinuous fibre while woven roving (WR) is a continuous fibre [25, 27, 28]. The two composites are formed when the fibre is bound with polyester resin or

epoxy resin [10, 23]. In this study, woven roving fiber is focused on and discussed in depth. Woven roving (WR) is built from a continuous strand of fiberglass roving as shown in Figure 1. The way woven roving is composed is similar to the ways yarns are woven in fabrics. Woven roving is heavier and thicker than fabric. It has a variety of weights and widths at 0.405 kg/m^2 to 1.36 kg/m^2 and 5 cm to 10 cm, respectively. Woven roving has maximum strength in all fibres direction, but the value is lower than a unidirectional mat [29].

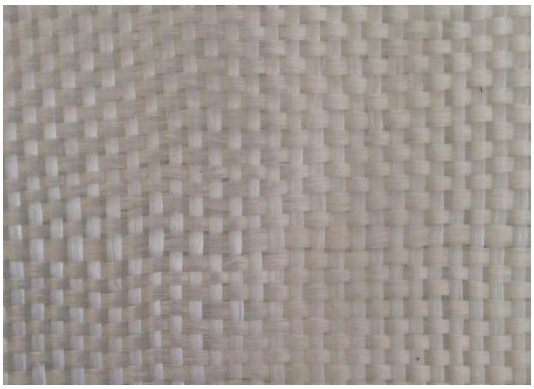

Figure 1**.** Woven Roving glass fibre single ply.

The aim of this project is to determine the failure strength, energy absorption and crushing behaviour of the composite square honeycomb structures. ABAQUS 6.13, a finite element analysis, are used to determine the numerical simulation of the honeycomb structure.

METHODS AMD MATERIALS

Mechanical Properties

The composites are formed when they were adhered with unsaturated polyester resin. The mechanical properties of reinforcement and matrix for glass fibre reinforced composites are shown in Table 1. The mechanical properties in Table 1 include Young's Modulus and Possion's ratio.[10].

Table 1. Mechanical properties of reinforcement and matrix [10].

Material	Young Modulus, *E* (GPa)	Poisson's Ratio, υ
Woven roving fabric	76	0.37
Polyester resin	3.5	0.25

Hand Lay-Up Method

Hand lay-up method is a simple and easy method to prepare a composite laminate as shown in Figure 2. First, the WR glass fibre is cut into the desired length. Each composite laminate consists of five layers of WR fibre ply. Before fabrication started, the glass plate and roller are cleaned by using acetone to remove the impurities that adhered on the composite laminates. After that, anti-adhesive agent is applied on the top of the glass plate to ease the composite removal process. A mixture of polyester resin and hardener (MEKP)

is weighted according to the amount needed. The first layer of WR is put on the glass plate and the mixture is poured onto the fibre. Then, the resin mixture is swept evenly throughout the fibre by using a roller. After the first layer of fibre ply is fully wetted by the mixture of resin, the next layer of fibre is added and the steps are repeated until five layers. After the hand lay-up process is completed, the specimen is left for 24 hours for the curing process. After the composite laminate is completed, the geometry of the control specimen is prepared according to the ASTM D3039 standard. ASTM D3039 is a standard test method used to measure the tensile properties of composite materials. The weights of the polyester resin and fibre used to fabricate the composition laminates are as shown in Table 2.

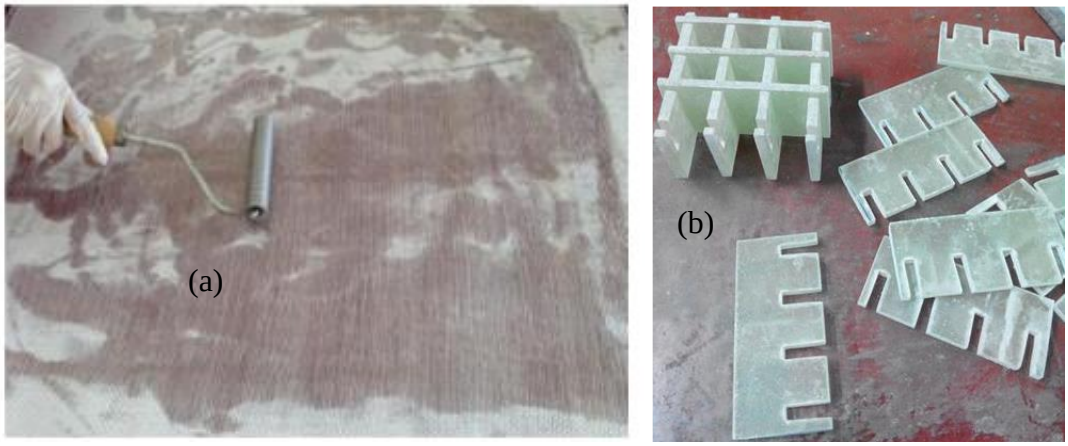

Figure 2. (a) Hand lay-up technique, (b) slotting technique.

Table 2. Weight of composition of composite laminate.

Weight of composition	(g)
WR fibre	615.4
Polyester resin	412.6

The property of the composite is influenced by the proportions of the matrix and fibre. The weight fraction of fibre can be expressed by eq. (1).

$$w_f = \frac{W_f}{W_c} \quad (1)$$

where, w_f = weight fraction of fibre; W_f = weight of fibre; W_c = weight of composite

Table 3 shows the composition of the composite laminate for WR fibre. The weight percentage of fibre, W_f is 60%, whereas the weight percentage of resin, W_m is 40% with a total weight of 1028g for the composite laminate. The weight fraction of fibre, w_f is 0.599.

Table 3. Composition of composite laminate.

Weight Percentage of Fibre, W_f(%)	Weight Percentage of Resin, W_m (%)	Weight Fraction of Fibre , w_f
60	40	0.599

Finite Element Modeling

Numerical models are developed to simulate the mechanical reponse of square honeycomb structure which is subjected to compression. In this simulation, woven roving composite is modelled as an isotropic material. However, due to the thin structure of the honeycomb core, the model will undergo buckling before the core fully collapsed. Therefore, to simulate exactly the collapse behaviour of the honeycomb core, a geometric with imperfection pattern is applied to the model. A geometric imperfection pattern is determined as a linear superposition of buckling eigenmodes acquired from a previous eigenvalue buckling prediction performed with Abaqus/Standard. Imperfections are ordinarily introduced by perturbations in the geometry [30]. There are three ways to determine imperfections such as a linear superposition of buckling eigenmodes, displacements of a static analysis and identifying the number of mode and imperfection values directly. In this project, the FEM analysis is carried out by using the *IMPERFECTION function in a linear perturbation step in Abaqus/Standard. The buckling modes are estimated and then a small imperfection is introduced in the straightness of the vertical cell members. If the imperfection is small, the deformation will be quite small (relative to the imperfection), below the critical load. The response will increase fast near the critical load, introducing a quick change in behaviour [30]. There are two ways of analysis to create the possible collapse modes by using Abaqus/Standard[31].

1. The first analysis is performed to obtain an eigenvalue of buckling with Abaqus/Standard on the "perfect" structure to get the possible collapse modes and to examine the mesh modes accurately.
2. The second analysis used Abaqus/Standard to introduce an imperfection in the geometry by adding buckling modes to the "perfect" geometry. The lowest buckling modes are frequently assumed to provide the most critical imperfections to create the perturbed mesh. The imperfection formula is as shown in eq. (2).

$$\Delta x_i = \sum_{i=1}^{M} w_i \emptyset_i \qquad (2)$$

where, $\emptyset_i$ is the i^{th} mode shape ; w_i is the associated scale factor.

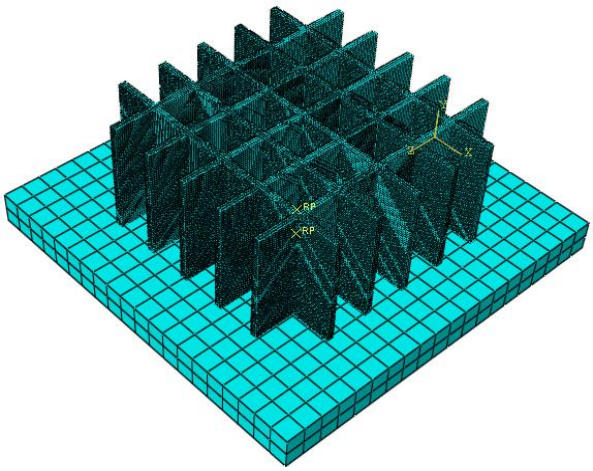

Figure 3**.** Meshes conditions for the square honeycomb cores.

The simplest buckling mode used to perturb the mesh and the scale factor is 0.00008 in the finite element models. The geometric imperfections in terms of the buckling modes are then imported into the Abaqus/Standard. The main reason of using imperfection in an analysis is to make brittle failure successful, which is correlative with the buckling collapse of the core cells [32]**.** The interaction between the loading platen and the face sheet is specified as a frictional contact and a general contact condition is generated between the individual web members. The honeycomb is meshed by 8-noded brick elements with reduced integration and the top and bottom loading platens are modelled as rigid bodies. Figure 3 shows the meshes conditions for the square honeycomb cores (the top platen has been removed). Load is applied through the top platen and the lower platen is fixed.

RESULTS AND DISCUSSION

Tensile Test Results

The tensile test is carried out until the specimen is fractured and the mechanical properties of the composite material are obtained. The results obtained for control specimens 1 and 2 are shown in Figure 4. It is shown that the load-displacement graph for the two control specimens depicted the same trend of the curve and the increase of the load is consistent. Specimen S2 achieved the higher force which is 11.7kN, whereas specimen S1 achieved a slightly lower force which is 10.95kN. The extension of displacement length for both specimens until fracture, S1 and S2 are 4mm and 4.10mm, respectively.

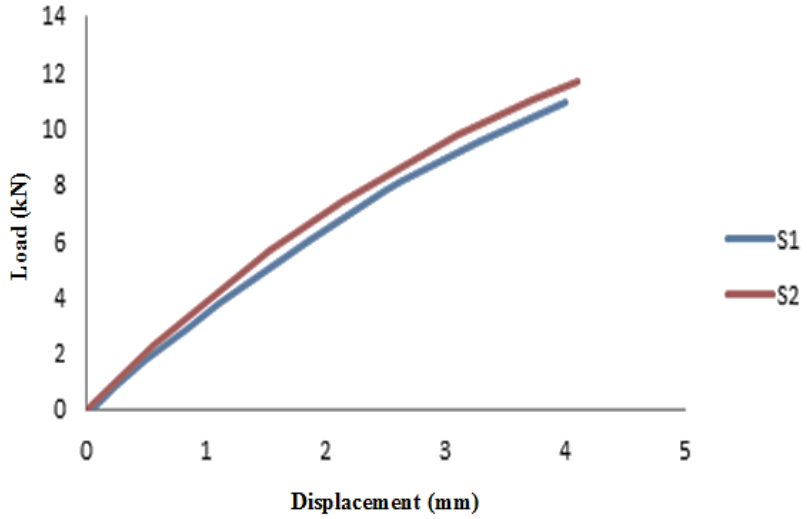

Figure 4**.** Load-displacement curve for control specimen.

Table 4**:** Summary of tensile test results for WR fibre

Specimen	Maximum Tensile stress (MPa)	Young's Modules (GPa)	Yield Stress (MPa)
S1	49.94	3.64	37.48
S2	50.53	3.77	40.49

The tensile test for both control specimens is summarised in Table 4. The maximum tensile stress for both specimens S1 and S2 are 49.94MPa and 50.53MPa, respectively. The Young's Modulus and Yield Strength for specimen S1 are 3.64GPa and 37.48MPa, respectively, whereas for specimen S2, the values are 3.77GPa and 40.49MPa respectively. There are no significant mechanical properties between both specimens. Therefore, the correlation between the two specimens is good.

Finite Element Analysis

There are three buckling modes of eigenvalues obtained on numerical simulation as shown in Figure 5. The eigenvalues obtained are 0.80763, 0.81466 and 0.81560 for the three buckling modes. The buckling modes are obtained and then introduced into the numerical simulation with a small imperfection to the vertical cell to straighten the cell members of the composite square honeycomb core structure[33].

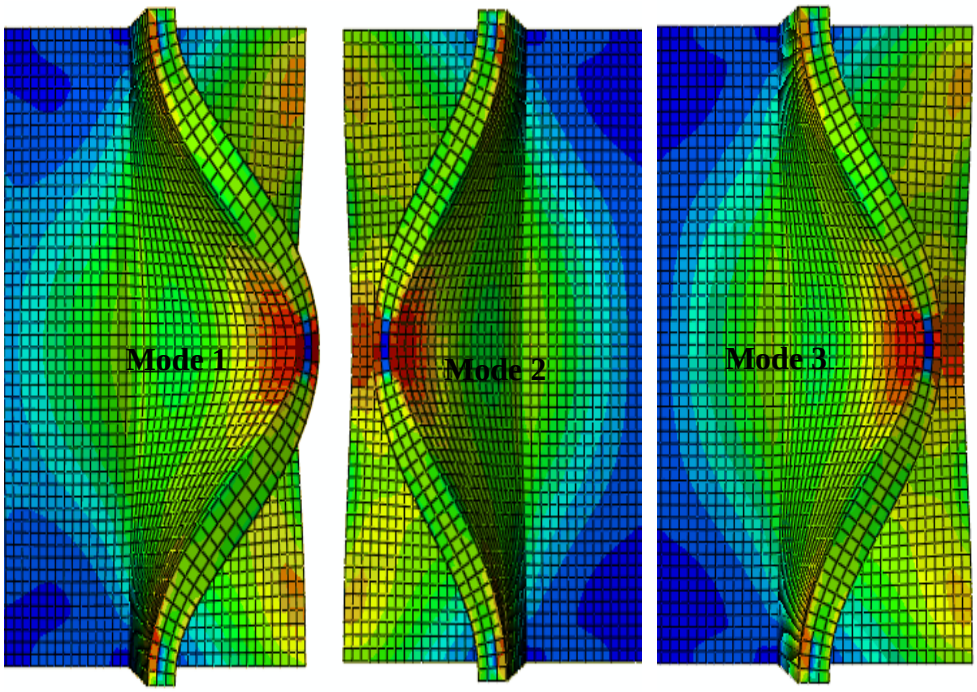

Figure 5. Eigenvalues, mode 1 = 0.80763, mode 2 = 0.81466, mode 3 = 0.81560.

Figure 6 shows a load-displacement curve for a compression test on the square honeycomb core structure. It can be noted that the stress is based on the total area of the square honeycomb structure, including the cells between the webs. The load-displacement curve increased rapidly during the elastic phase before achieving the maximum stress, and the curve dropped rapidly once the square honeycomb core structure started to buckle. After the square honeycomb core structure began to buckle, the region is called as the plastic phase [34]. Figure 7 shows a compressed structure and focus area of the maximum stress of composite square honeycomb structure after undergoing compression. The stress is based on the total area of the structure. Based on the simulation, the maximum stress obtained is 28.24 MPa. The maximum stress is obtained once the composite square honeycomb structure is crushed to 16 mm. Table 5 shows the stress distributed along the maximum node. Along the maximum node, the stress range is

between 27.76MPa to 28.24MPa. Based on the numerical simulation, the maximum stress obtained is 28.24MPa which is located at node 110451.

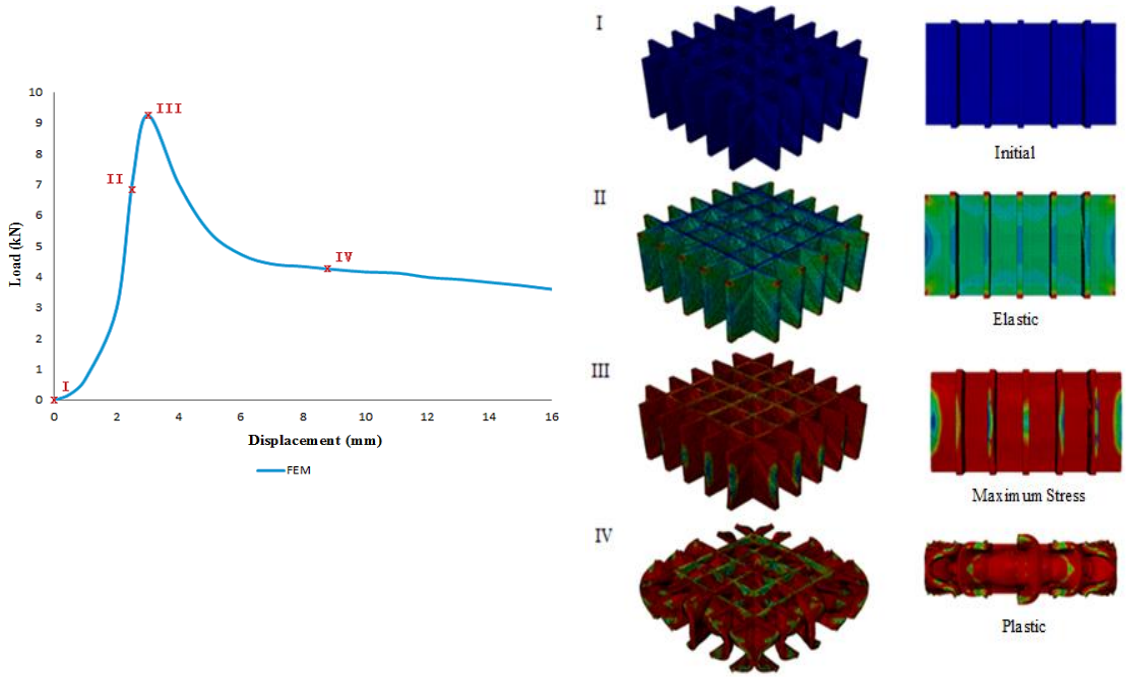

Figure 6. Load-displacement curve for FEM analysis.

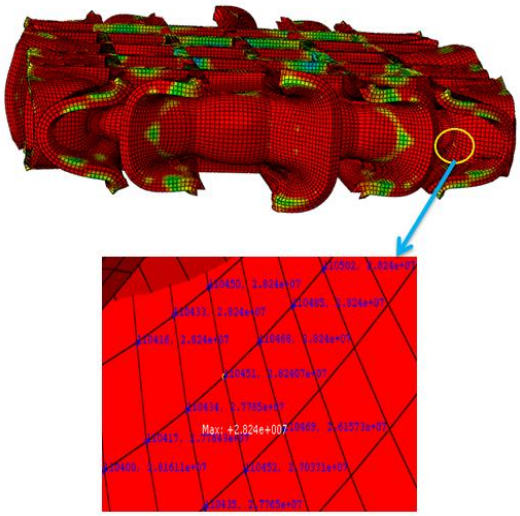

Figure 7. Maximum stress on compressed structure.

Table 5. Stress along the maximum node.

Node	Stress (MPa)
110400	28.16
110417	27.76
110434	27.77
110451	28.24

Comparison between Analytical and Experimental Results

Energy Absorption

One of the most important applications of composite square honeycomb core structure is high energy absorbing structure. In this project, the energy absorption of the structure is determined from the energy under the load-displacement curve. Figure 8 shows a comparison of the experimental and numerical load-displacement curves for the composite square honeycomb structure. In general, the correlation between experimental and numerical results is excellent with all the main features of initial, elastic, maximum stress and plastic region. The peak load for both results is almost the same and they have achieved a good agreement in the load-displacement curve.

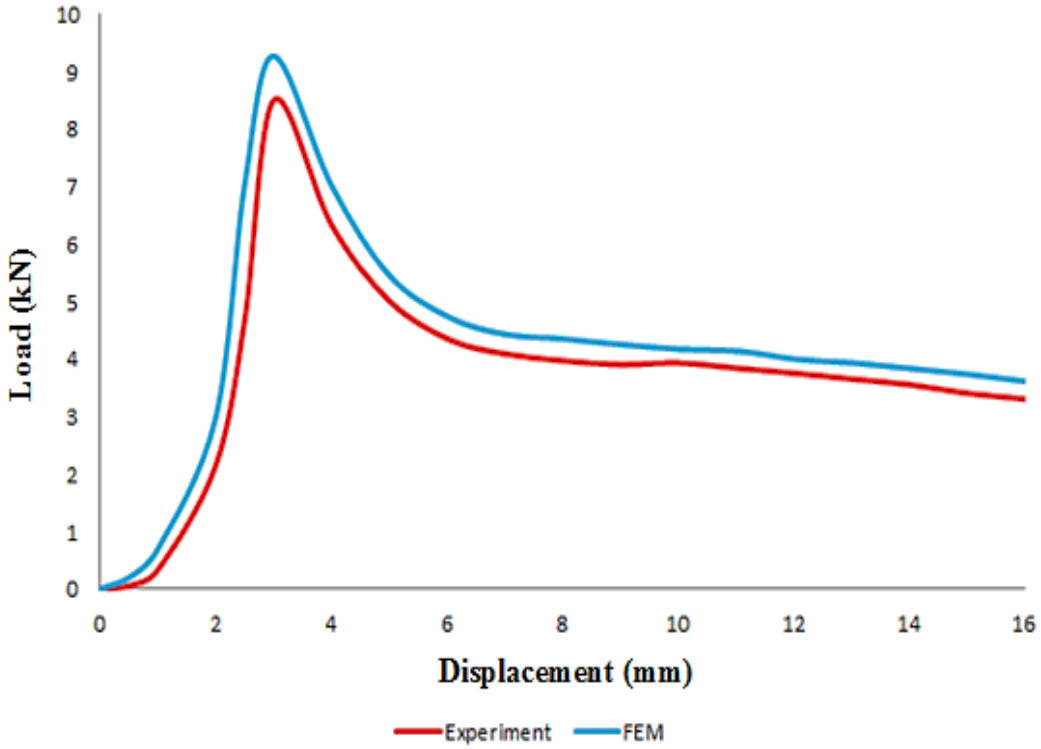

Figure 8. Load-displacement curves for experimental and finite element results.

Table 6 shows the percentage error between FEM and the experimental results. The energy absorption of finite element result is slightly higher compared to the experimental result. This is because the finite element model is assumed to be a perfect structure, whereas in the experimental model, there is an imperfection on the geometric during the fabrication process. The percentage error is 9.23%, which can be considered as a good agreement between the simulation and experimental results.

Table 6**.** Discrepancy between FEM and experiment results.

Energy Absorption (kJ)		Percentage
FEM	Experimental	of error (%)
310.86	282.17	9.23

Crushing Behaviour

Figure 9 shows the crushing behaviour of composite square honeycomb core structure after being compressed under different displacements. The left figure is the finite element model, while the right figure is the experimental model of the composite square honeycomb core structure. For the first two diagrams, both models are showing a very good agreement for the crushing behaviour; whereas for the last four diagrams, when the vertical cells started to buckle, the crushing behaviour is different to each other. When the structure is being compressed, the vertical cell for the finite element model is symmetrical whereas for the experimental model, the vertical cell is buckled to the left side. The finite element and experimental models are slightly different to each other due to the imperfection of geometric during fabrication of the specimens. The geometric in the simulation is assumed as the preferred structure.

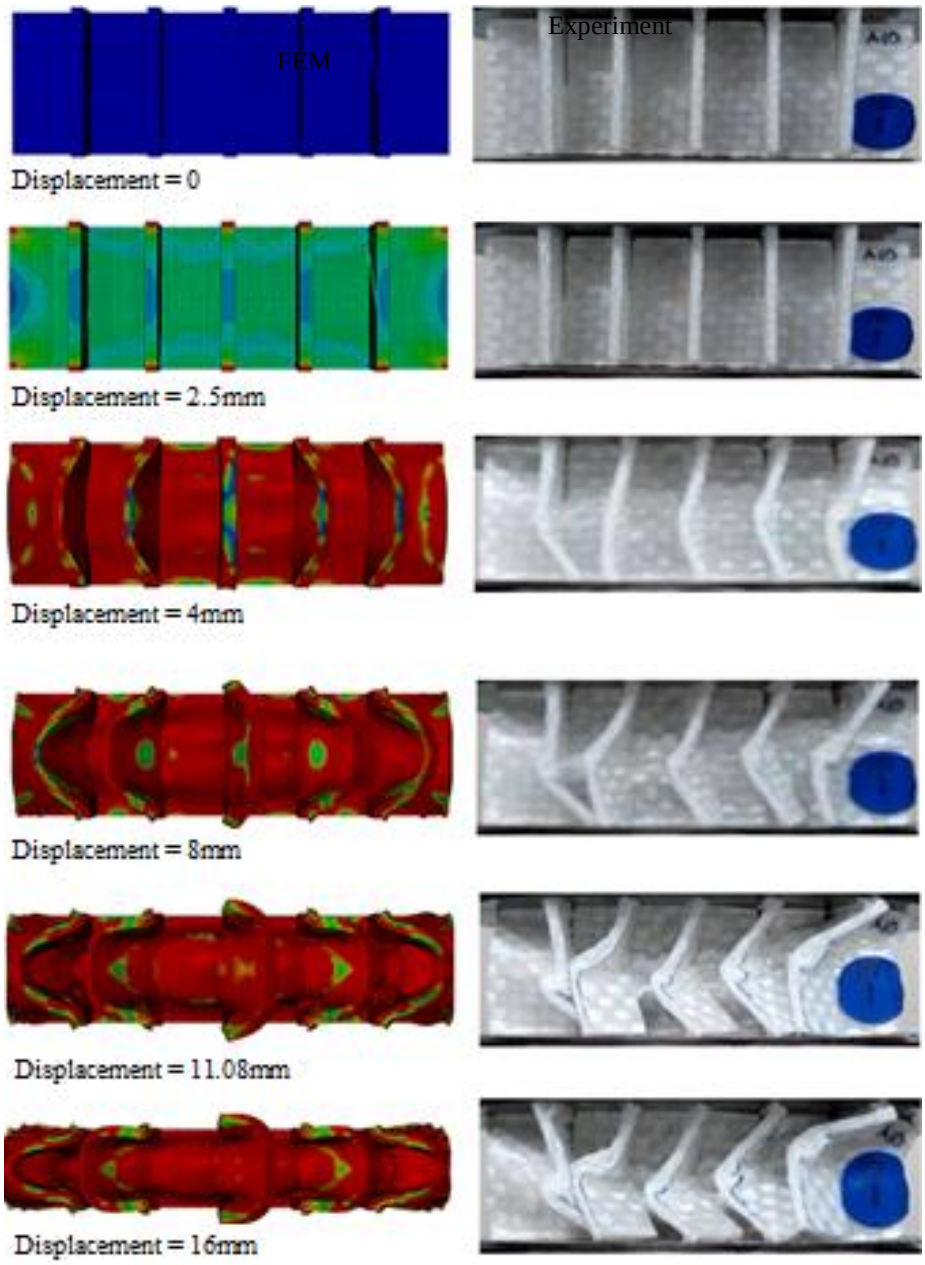

Figure 9. Crushing behaviour for FEM and experimental data.

CONCLUSIONS

Honeycomb structure is widely used in various sectors such as the automotive and aerospace industries. This structure has high energy absorption, is lightweight, fire resistant, has low density and high strength to weight ratio; therefore, it is suitable in designing a vehicle. In this project, the woven roving fibre and polyester resin are chosen to fabricate the composite laminate. The mechanical properties of the control specimens are determined by using ASTM D3039. The results of Young's Modulus and Yield Stress obtained are 3.77GPa and 40.49 MPa, respectively. There are three buckling modes of eigenvalues result obtained from a numerical simulation which are 0.80763 0.81466 and 0.81560 for mode 1, mode 2 and 3 respectively. The maximum stress obtained from the numerical simulation is 28.24MPa which is located at node 110451. Besides that, the absorption energy for finite element and experimental results are 310.86 kJ and 282.17 kJ respectively. The percentage of error is 9.23% which can be considered a good agreement between the numerical simulation and experimental data. Lastly, the crushing behaviour between the finite element model and experimental model is slightly different to each other because the model in the simulation is assumed to be the preferred structure whereas the experimental model is imperfect in the geometric. As a conclusion, the objectives of the project have been succefully achieved, which are to analyse the crushing behaviour of square honeycomb structure by using FEM software, to determine the failure strength and energy absorption of square honeycomb structure by using FEM software and to compare between the FEM results and experimental data from the compression test.

ACKNOWLEDGEMENTS

The authors would like to express their thanks to the Universiti Malaysia Pahang for funding this project (RDU1403109).

REFERENCES

[1] Li M, Deng Z-q, Guo H-w, Liu R-q, Ding B-c. Optimizing crashworthiness design of square honeycomb structure. Journal of Central South University. 2014;21:912-9.

[2] Wan Dalina WAD, Mariatti M, Mohd Ishak ZA, Mohamed AR. Comparison of properties of mwcnt/carbon fibre/ epoxy laminated composites prepared by solvent spraying method. International Journal of Automotive and Mechanical Engineering. 2014;10:1901-9.

[3] Ravi Sankar H, Srikant RR, Vamsi Krishna P, Bhujanga Rao V, Bangaru Babu P. Estimation of the dynamic properties of epoxy glass fabric composites with natural rubber particle inclusions. International Journal of Automotive and Mechanical Engineering. 2013;7:968-80.

[4] Karakoç A, Freund J. A statistical failure initiation model for honeycomb materials. Composite structures. 2013;95:154-62.

[5] Nazirah ZS, Abdul Majid MS, Daud R. Effects of elevated temperatures on glass-reinforced epoxy pipes under multi-axial loadings. Journal of Mechanical Engineering and Sciences. 2016;10:1846-56.

[6] Fairuz AM, Sapuan SM, Zainudin ES, Jaafar CNA. Effect of filler loading on mechanical properties of pultruded kenaf fibre reinforced vinyl ester composites. Journal of Mechanical Engineering and Sciences. 2016;10:1931-42.

[7] Abdul Majid MS, Daud R, Afendi M, Amin NAM, Cheng EM, Gibson AG, et al. Stress-strain response modelling of glass fibre reinforced epoxy composite pipes under multiaxial loadings. Journal of Mechanical Engineering and Sciences. 2014;6:916-28.
[8] Shen C, Lu G, Yu T. Dynamic behavior of graded honeycombs–a finite element study. Composite structures. 2013;98:282-93.
[9] Asprone D, Auricchio F, Menna C, Morganti S, Prota A, Reali A. Statistical finite element analysis of the buckling behavior of honeycomb structures. Composite structures. 2013;105:240-55.
[10] Arifin A, Abdullah S, Rafiquzzaman M, Zulkifli R, Wahab D. Failure characterisation in polymer matrix composite for un-notched and notched (open-hole) specimens under tension condition. Fibers and Polymers. 2014;15:1729-38.
[11] Jones RM. Mechanics of composite materials: CRC press; 1998.
[12] Sutherland L, Soares CG. Impact tests on woven-roving e-glass/polyester laminates. Composites Science and Technology. 1999;59:1553-67.
[13] Kolawole MY, Aweda JO, Abdulkareem S. Archachatina marginata bio-shells as reinforcement material in metal matrix composites. International Journal of Automotive and Mechanical Engineering. 2017;14:4068-79.
[14] Ahmed S, Ahsan A, Hasan M. Physico-mechanical properties of coir and jute fibre reinforced hybrid polyethylene composites. International Journal of Automotive and Mechanical Engineering. 2017;14:3927-37.
[15] Fatchurrohman N, Sulaiman S, Sapuan SM, Ariffin MKA, Baharuddin BTHT. Analysis of a metal matrix composites automotive component. International Journal of Automotive and Mechanical Engineering. 2015;11:2531-40.
[16] Gdoutos EE, Pilakoutas K, Rodopoulos C. Failure analysis of industrial composite materials: McGraw-Hill Professional; 2000.
[17] Then YY, Ibrahim NA, Zainuddin N, Ariffin H, Wan Yunus WMZ, Abd Rahman MF. Effect of electron beam irradiation on the tensile properties of oil palm mesocarp fibre/poly(butylene succinate) biocomposites. International Journal of Automotive and Mechanical Engineering. 2014;10:2070-80.
[18] Othman RN, Wilkinson AN. The impedance characterization of hybrid cnt-silica epoxy nanocomposites. International Journal of Automotive and Mechanical Engineering. 2014;10:1832-40.
[19] Mohamad M, Marzuki HFA, Bakar SNA, Abdullah AN, Ubaidillah EAE, Abidin MFZ, et al. Effect of anodizing electrolyte for structural adhesives bonding study of aluminium-carbon laminates composites. International Journal of Automotive and Mechanical Engineering. 2014;10:2091-101.
[20] Maleque MA, Radhi M, Rahman MM. Wear study of mg-sicp reinforcement aluminium metal matrix composite. Journal of Mechanical Engineering and Sciences. 2016;10:1758-64.
[21] Kalpakjian S. Manufacturing engineering and technology (6th ed in si unit)2010.
[22] Ahmad R, Ajer MR. Investigation of epoxy powder coated galvanized steel substrate through electrostatic powder coating system. International Journal of Automotive and Mechanical Engineering. 2015;11:2622-38.
[23] Ismail AE, Che Abdul Aziz MA. Tensile strength of woven yarn kenaf fiber reinforced polyester composites. Journal of Mechanical Engineering and Sciences. 2015;9:1695-704.

[24] Ibrahim MS, Sapuan SM, Faieza AA. Mechanical and thermal properties of composites from unsaturated polyester filled with oil palm ash. Journal of Mechanical Engineering and Sciences. 2012;2:133-47.
[25] Hamdan S, Kiew KS, Rahman MR. Dielectric properties of maleic anhydride modified unsaturated polyester composites reinforced with chicken feather fibre. International Journal of Automotive and Mechanical Engineering. 2014;10:1971-9.
[26] Lubin G. Handbook of composite materials. Van Nostrand Reinhold Co; 1982.
[27] Hafizi ZM, Epaarachchi J, Lau KT. An investigation of acoustic emission signal attenuation for monitoring of progressive failure in fiberglass reinforced composite laminates. International Journal of Automotive and Mechanical Engineering. 2013;8:1442-56.
[28] Jeffrey KJT, Tarlochan F, Rahman MM. Residual strength of chop strand mats glass fiber/epoxy composite structures: Effect of temperature and water absorption. International Journal of Automotive and Mechanical Engineering. 2011;4:504-19.
[29] Chan WT. The effects of fibre volume fraction of composite plate: Universiti Malaysia Pahang; 2007.
[30] Tawfik S, Tan X, Ozbay S, Armanios E. Anticlastic stability modeling for cross-ply composites. Journal of Composite Materials. 2007;41:1325-38.
[31] Rejab M, Cantwell W. The mechanical behaviour of corrugated-core sandwich panels. Composites Part B: Engineering. 2013;47:267-77.
[32] Hibbitt K. Abaqus: User's manual: Version 6.13: Hibbitt. Karlsson & Sorensen, Incorporated. 2013.
[33] Rejab M, Ushijima K, Cantwell W. The shear response of lightweight corrugated core structures. Journal of Composite Materials. 2013:0021998313514086.
[34] Zuhri MYM, Guan ZW, Cantwell WJ. The mechanical properties of natural fibre based honeycomb core materials. Composites Part B: Engineering. 2014;58:1-9.